JOC Article
pubs.acs.org/joc

Competitive Intramolecular Hydrogen Bonding in Oligo(ethylene oxide) Substituted Quadruple Hydrogen Bonded Systems

Tom F. A. de Greef, Marko M. L. Nieuwenhuizen, Rint P. Sijbesma,* and E. W. Meijer*

Institute for Complex Molecular Systems and Laboratory of Macromolecular and Organic Chemistry, Eindhoven University of Technology, P.O. Box 513, 5600 MB Eindhoven, The Netherlands

r.p.sijbesma@tue.nl; e.w.meijer@tue.nl

Received October 3, 2009

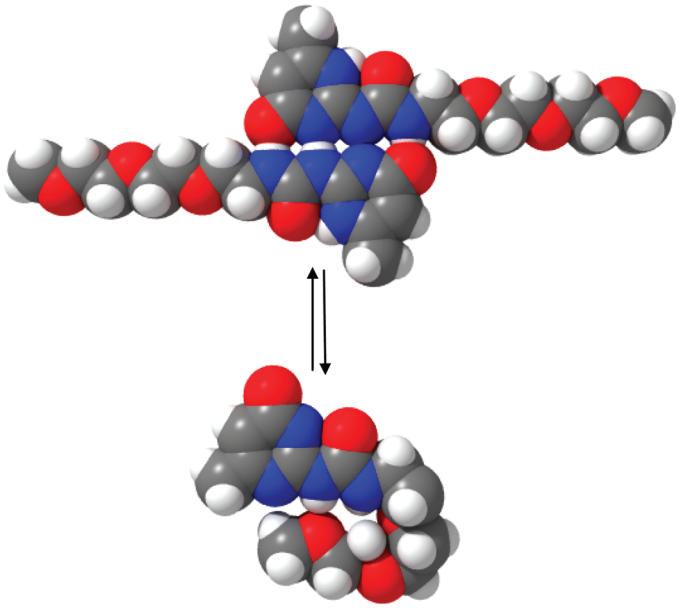

A series of oligo(ethylene oxide) (oligoEO) substituted 2-ureido-pyrimidinones (UPy), differing in the number of ethylene oxide units and the length of the aliphatic spacer connecting the oligoEO side chain with the UPy group, have been prepared. It was found that variation in these structural parameters strongly influences the dimerization constant (K_{dim}) of the UPy dimer and the association constant (K_a) of UPy with 2,7-diamido-1,8-naphthyridine (NaPy) in chloroform. By analyzing the relation between dimerization strength, length of aliphatic spacer, and the number of EO units in the oligoEO chain, we present strong evidence that the reduction in hydrogen bond strength is caused by competitive intramolecular hydrogen bonding of the ether atoms of the oligoEO chain to the hydrogen bond donors of the UPy unit.

Introduction

Polar side chains such as oligo(ethylene oxides) (oligoEO) are widely employed as solubilizing chains for the construction of supramolecular assemblies in water.[1] Supramolecular polymers[2] and networks[3] based on hydrogen bonding have been created using a combination of polar and apolar polymers that serve both as linking units to physically connect the associating end groups and as structurally organizing units due to the incompatibility of hydrophilic and hydrophobic chains.[4] Because of their low toxicity and excellent biocompatibility, oligoEO chains are also applied in the design of low-molecular-weight hydrogelators[5] and multivalent ligands.[6]

However, substitution of supramolecular assemblies with polar oligomers and polymers can lead to unexpected results. For example, Kaifer[7] reported a generation-dependent drop in the dimerization constant of quadruple hydrogen-bonded ureido-pyrimidinone dimers substituted with polar

Published on Web 01/11/2010 DOI: 10.1021/jo902053t

Newkome-type oligoamide dendrons. The large drop in dimerization strength on going from the first (G_1, $K_{dim} > 10^6$ M^{-1}) to the third generation (G_3, K_{dim} = 2.6 M^{-1}) dendron was attributed to either an increase in the steric hindrance exerted by the larger dendritic component or by the increase in the relative polarity of the microenvironment created by the dendritic wedge. In contrast to the results obtained by Kaifer, Chow and co-workers[8] reported a generation-independent (G_1-G_3) dimerization constant of 2-ureido-pyrimidinones equipped with less polar Fréchet-type oligo arylether dendrons.[8] Because the oligoamide G_3 dendron is approximately similar in size compared to the oligo arylether G_3 dendron, these authors conclude that the decrease in dimerization strength, as observed in the study by Kaifer and co-workers, is a result of an increase in the polarity of the microenvironment, which directly influences the strength of the individual hydrogen bonds. Although the increase in the polarity of the microenvironment seems a plausible explanation for the observed decrease in dimerization strength, it must be noted that a generation-dependent increase in the polarity of the microenvironment has been measured for oligo arylether dendrons.[9] An alternative explanation for the large decrease in dimerization strength, which has not been noted by the authors, is hydrogen-bond-induced backfolding of the polar side chains to the polar groups of the 2-ureido-pyrimidinone moiety. Hydrogen-bond-induced backfolding of end groups is commonly observed in various polar dendrimers such as PPI and PAMAM dendrimers in both apolar and polar solvents.[10] In this respect, the large difference between substitution with polar oligoamide dendrons and substitution with apolar oligoaryl ether dendrons on the UPy dimerization strength can also be explained by the more flexible character of the oligoamide dendrons compared to the more rigid oligoaryl ether dendrons and by the fact that the oligoamide dendron contains stronger hydrogen bond donors and acceptors capable of intramolecular competition with the quadruple hydrogen bond array of the UPy dimer.

Several other examples can be found in the literature confirming the active participation of oligoEO chains in the self-assembly of various supramolecular structures. For example, Stoddart and co-workers reported[11] a stabilizing effect of oligoEO chains on the complexation of cyclobis(paraquat-*p*-phenylene) with a 1,4-dioxybenzene-based acyclic guest. The values of the association constants (K_a) of the corresponding complexes varied significantly depending on the nature of the substituents attached to the aromatic ring of the 1,4-dioxybenzene guest. Attachment of long oligoEO chains resulted in a significant increase (10^2) in association constant compared to short oligoEO chains, presumably due to favorable [CH···O] interactions between the polyether oxygen atoms and acidic hydrogen atoms located on the bipyridinium units of the host.[11] Bouteiller and co-workers reported[12] on the hydrogen-bonded supramolecular polymerization of oligoEO substituted bis-urea monomers in water, toluene, and acetonitrile. It was found that direct attachment of the oligoEO chain to the bis-urea monomer resulted in low viscosity solutions in toluene, indicating that only small supramolecular oligomers are formed in this solvent. Introduction of a larger aliphatic spacer between the urea protons and the oligoEO resulted in solutions of much higher viscosity in toluene at the same concentration, indicating that the association constant of the monomer is increased considerably as a result of the presence of the larger aliphatic spacer. These and other[13] examples clearly demonstrate the remarkable effect of the attachment of short oligoEO chains on the thermodynamics of supramolecular assemblies.

(1) (a) Hirschberg, J. H. K. K.; Brunsveld, L.; Ramzi, A.; Vekemans, J. A. J. M.; Sijbesma, R. P.; Meijer, E. W. *Nature* **2000**, *402*, 167. (b) Brunsveld, L.; Vekemans, J. A. J. M.; Hirschberg, J. H. K. K.; Sijbesma, R. P.; Meijer, E. W. *Proc. Natl. Acad. Sci. U.S.A.* **2002**, *99*, 4977. (c) Brunsveld, L.; Lohmeijer, B. G. G.; Vekemans, J. A. J. M.; Meijer, E. W. *Chem. Commun.* **2000**, 2305. (d) Sinkeldam, R. W.; van Houtem, M. H. C. J.; Pieterse, K.; Vekemans, J. A. J. M.; Meijer, E. W. *Chem.—Eur. J.* **2006**, *12*, 6129. (e) Mathews, J. R.; Goldoni, F.; Schenning, A. P. H. J.; Meijer, E. W. *Chem. Commun.* **2005**, 5503. (f) Kilbinger, A. F. M.; Schenning, A. P. H. J.; Goldoni, F.; Feast, W. J.; Meijer, E. W. *J. Am. Chem. Soc.* **2000**, *122*, 1820. (g) Wolffs, M.; Hoeben, F. J. M.; Beckers, E. H. A.; Schenning, A. P. H. J.; Meijer, E. W. *J. Am. Chem. Soc.* **2005**, *127*, 13484. (h) Arnaurd, A.; Belleney, J.; Boué, F.; Bouteiller, L.; Carrot, G.; Wintgens, V. *Angew. Chem., Int. Ed.* **2004**, *43*, 1718. (i) Harada, A.; Cammas, S.; Kataoka, K. *Macromolecules* **1998**, *29*, 6183. (j) Schmuck, C.; Wienand, W. *J. Am. Chem. Soc.* **2003**, *125*, 452. (k) Schmuck, C.; Frey, P.; Heil, M. *ChemBioChem* **2005**, *6*, 628. (l) Schmuck, C.; Rehm, T.; Gröhn, F.; Klein, K.; Reinhold, F. *J. Am. Chem. Soc.* **2006**, *128*, 1430. (m) Inoue, Y.; Kuad, P.; Okumura, Y.; Takashima, Y.; Yamaguchi, H.; Harada, A. *J. Am. Chem. Soc.* **2006**, *129*, 6396. (n) Inoue, Y.; Miyauchi, M.; Nakajima, H.; Takashima, Y.; Yamaguchi, H.; Harada, A. *Macromolecules* **2007**, *40*, 3256. (o) Lee, M.; Lee, S.-J.; Jiang, L.-H. *J. Am. Chem. Soc.* **2004**, *126*, 12724. (p) Kim, B.-S.; Hong, D.-J.; Bae, J.; Lee, M. *J. Am. Chem. Soc.* **2005**, *127*, 16333. (q) Bae, J.; Choi, J.-H.; Yoo, Y.-S. ; Oh, N.-K.; Kim, B.-S. ; Lee, M. *J. Am. Chem. Soc.* **2005**, *127*, 9668. (r) Stone, M. T.; Moore, J. S. *Org. Lett.* **2004**, *6*, 469. (s) Ryu, J.-H.; Hong, D.-J.; Lee, M. *Chem. Commun.* **2008**, 1043. (t) Jiang, J.; Tew, G. *Org. Lett.* **2008**, *10*, 4393. (u) Xu, Y.-X.; Wang, G.-T.; Zhao, X.; Jiang, X.-K.; Li, Z.-T. *Langmuir* **2009**, *25*, 2684. (v) Seo, S. H.; Chang, J. Y.; Tew, G. N. *Angew. Chem., Int. Ed.* **2006**, *118*, 7688. (w) Fernández, G.; García, F.; Sánchez, L. *Chem. Commun.* **2008**, 6567.

(2) Lafitte, V. G. H.; Aliev, A. E.; Horton, P. N.; Hursthouse, M. B.; Bala, K.; Golding, P.; Hailes, H. C. *J. Am. Chem. Soc.* **2006**, *128*, 6544.

(3) Binder, W. H.; Petraru, L.; Roth, T.; Groh, P. W.; Pálfi, V.; Keki, S.; Ivan, B. *Adv. Funct. Mater.* **2007**, *17*, 1317.

(4) (a) Yang, X.; Hua, F.; Yamato, K.; Ruckenstein, E.; Gong, B.; Kim, W.; Ryu, C. Y. *Angew. Chem., Int. Ed.* **2004**, *43*, 6471. (b) Feldman, K. E.; Kade, M. J.; de Greef, T. F. A.; Meijer, E. W.; Kramer, E. J.; Hawker, C. J. *Macromolecules* **2008**, *41*, 4694. (c) Tang, C.; Lennon, E. M.; Fredrickson, G. H.; Kramer, E. J.; Hawker, C. J. *Science* **2008**, *322*, 429.

(5) (a) van Bommel, K. J. C.; van der Pol, C.; Muizebelt, I.; Friggeri, A.; Heeres, A.; Meetsma, A.; Feringa, B.; van Esch, J. *Angew. Chem., Int. Ed.* **2004**, *43*, 1663. (b) Friggeri, A.; van der Pol, C.; van Bommel, K. J. C.; Heeres, A.; Stuart, M. C. A.; Feringa, B. L.; van Esch, J. *Chem.—Eur. J.* **2005**, *11*, 5353.

(6) (a) Mammen, M.; Choi, S.-K.; Whitesides, G. M. *Angew. Chem., Int. Ed.* **1998**, *37*, 2755. (b) Bilgicer, B.; Moustakas, D. T.; Whitesides, G. M. *J. Am. Chem. Soc.* **2007**, *129*, 3722. (c) Krishnamurthy, V. M.; Semetey, V.; Bracher, P. J.; Shen, N.; Whitesides, G. M. *J. Am. Chem. Soc.* **2007**, *129*, 1312. (d) Crespo-Biel, O.; Lim, C. W.; Ravoo, B. J.; Reinhoudt, D. N.; Huskens, J. *J. Am. Chem. Soc.* **2006**, *128*, 17024. (e) Mulder, A.; Auletta, T.; Sartori, A.; Del Ciotto, S.; Casnati, A.; Ungaro, R.; Huskens, J.; Reinhoudt, D. N. *J. Am. Chem. Soc.* **2004**, *126*, 6627. (f) Kiessling, L.; Gestwicki, J. E.; Strong, L. E. *Curr. Opin. Chem. Biol.* **2004**, *4*, 696.

(7) Sun, H.; Kaifer, A. E. *Org. Lett.* **2005**, *7*, 3845.

(8) Wong, C.-H. ; Chow, H.-F.; Hui, S.-K.; Sze, K.-H. *Org. Lett.* **2006**, *8*, 1811.

(9) Hawker, C. J.; Wooley, K. L.; Fréchet, J. M. J. *J. Am. Chem. Soc.* **1993**, *115*, 4375.

(10) (a) Chai, M.; Niu, Y.; Youngs, W. J.; Rinaldi, P. L. *J. Am. Chem. Soc.* **2001**, *123*, 4670. (b) Lin, C.; Wu, K.; Sa, R.; Mang, C.; Liu, P.; Zhuang, B. *Chem. Phys. Lett.* **2002**, *363*, 343. (c) Maiti, P. K.; Çağin, T.; Lin, S.-T.; Goddard, W. A. III *Macromolecules* **2005**, *38*, 979.

(11) Gillard, R. E.; Raymo, F. M.; Stoddart, J. F. *Chem.—Eur. J.* **1997**, *12*, 1933 and references therein.

(12) Obert, E.; Bellot, M.; Bouteiller, L.; Andrioletti, F.; Lehen-Ferrenbach, C.; Boué, F. *J. Am. Chem. Soc.* **2007**, *129*, 15601.

(13) Other examples on the effect of short EO chains on hydrogen bonding based self-assemblies: (a) Nygaard, S.; Hansen, C. N.; Jeppesen, J. O. *J. Org. Chem.* **2007**, *72*, 1617. (b) Hofacker, A. L.; Parquette, J. R. *Angew. Chem., Int. Ed.* **2005**, *44*, 1053. (c) Yoshikawa, I.; Sawayama, J.; Araki, K. *Angew. Chem., Int. Ed.* **2008**, *47*, 1038. (d) Stals, P. J. M.; Haveman, J. F.; Martin, R.; Fitié, C. F. C.; Palmans, A. R. A.; Meijer, E. W. *J. Mater. Chem.* **2009**, *19*, 124.

CHART 1. Design and Structure of Ethylene Oxide Substituted 2-Ureido-pyrimidinones 1a−1g

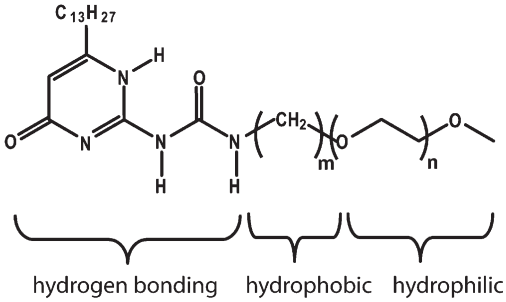

1a : n = 0 m = 2
1b : n = 0 m = 3
1c : n = 1 m = 2
1d : n = 1 m = 3
1e : n = 2 m = 2
1f : n = 2 m = 3
1g : n = 2 m = 6

Recently we reported on the effect of a short oligoEO chain on the dimerization constant (K_{dim}) of quadruple hydrogen-bonded dimers of 2-ureido-pyrimidinone in the apolar solvent chloroform.[14] Specifically, it was shown that substitution of the UPy monomer with a short tri(ethylene glycol) chain, connected *via* a C_2 aliphatic spacer to the ureido group, results in a drop of the dimerization constant by a factor of 2000 in chloroform. In contrast, no evidence for a reduction in dimerization strength was found when the tri(ethylene glycol) chain was connected *via* a larger C_6 aliphatic spacer. Because the 2-ureido-pyrimidinone unit is used in the construction of supramolecular materials where it serves as a physical chain-extending and cross-linking moiety, it is of utmost importance to characterize the conditions by which polar oligomers (such as oligoEO) and polymers covalently attached to the UPy unit could enhance or decrease the material properties by changing the dimerization strength or association dynamics. Furthermore, because of the synthetic accessibility of the UPy monomer and the detailed knowledge of its tautomerization[15] and dimerization equilibria,[16] the UPy system provides an ideal model system to study the relationship between dimerization strength, length of the aliphatic spacer, and the number of ethylene oxide units in the polar side chain. In this paper we present a detailed investigation on the relation between these three variables and by doing so find evidence that the reduction in dimerization strength is caused by hydrogen-bond-induced backfolding of the oligoEO chain to the ureido NH protons of the UPy monomer.

Results and Discussion

Synthesis and Design. To study the effect of short oligoEO chains on UPy dimerization strength, a series of UPy monomers **1a−1g** were synthesized (Chart 1).

Each UPy monomer consists of the following parts:

1. *The UPy group, capable of quadruple hydrogen-bonding interactions*.Previously, the dimerization constant of this unit, substituted with aliphatic substituents at the ureido group, was determined to be 6×10^7 M^{-1} in $CHCl_3$.[16]
2. *An apolar alkylene spacer linking the oligoEO chain with the UPy group*.Large alkylene spacers provide both a low polarity microenvironment as well as a significant entropic barrier for backfolding of the oxygen atoms of the oligoEO chain to the acidic NH protons of the ureido functionality of the UPy monomer. Intramolecular hydrogen bonding of the oxygen atoms of the oligoEO chain to the acidic NH protons of the UPy unit will result in a loss of conformational freedom of the alkylene spacer, which in turn results in an increasing conformational entropy across the series $m = 2, 3, 6$ (see Chart 1). It has been estimated by Page, Jencks[17] and Mandolini[18] that the entropy that is lost by freezing one methylene group is approximately 4−4.5 cal/K for nonsubstituted alkanes. Although entropic effects are important in reversible cyclizations, enthalpic effects such as the enthalpic contribution of the intramolecular hydrogen bond[19] and torsional strain[20] caused by an increase in the number of unfavorable *gauche* interactions upon backfolding of the alkylene spacer are of equal importance.
3. *A hydrophilic ethylene oxide substituent containing various numbers of oxygen ether type hydrogen bond acceptors connected to the alkyl spacer*.FT-IR measurements on the monoalkyl ethers of ethylene glycol ($n = 0-3$) in $CHCl_3$ have shown that the number of conformations in which an intramolecular hydrogen bond is present between the free OH and the oxygen atoms increases as the number of ethylene oxide units is increased.[21] Because the urea functionality contains two acidic NH protons capable of hydrogen bonding with the hydrogen-bond-accepting oxygen atoms of the oligoEO chain, a large difference in K_{dim} is expected upon increasing n.

The synthesis of the substituted 2-ureido-pyrimidinones **1a−g** is straightforward and based on sequences introduced

(14) de Greef, T. F. A.; Nieuwenhuizen, M. M. L.; Stals, P. J. M.; Fitié, C. F. C.; Palmans, A. R. A.; Sijbesma, R. P.; Meijer, E. W. *Chem. Commun.* **2008**, 4306.
(15) Beijer, F. H.; Sijbesma, R. P.; Kooijman, H.; Spek, A. L.; Meijer, E. W. *J. Am. Chem. Soc.* **1998**, *120*, 6761.
(16) Söntjens, S. H. M.; Sijbesma, R. P.; van Genderen, M. H. P.; Meijer, E. W. *J. Am. Chem. Soc.* **2000**, *122*, 7487.
(17) (a) Page, M. I.; Jencks, W. P. *Proc. Natl. Acad. Sci. U.S.A.* **1971**, *68*, 1678. (b) Page, M. I. *Chem. Soc. Rev.* **1973**, *2*, 295.
(18) Mandolini, L. *Adv. Phys. Org. Chem.* **1986**, *22*, 1.
(19) The enthalpic contribution of the intramolecular hydrogen bond is largely dependent on the strength and spatial juxtaposition of the hydrogen bond donor and acceptor. The strength of the intramolecular hydrogen bond formed between the oxygen atoms of the EO chain and the urea NH proton is much lower compared to a normal amide-amide hydrogen bond due to the fact that the carbonyl group is a better electron donor for hydrogen bonding than the ether oxygen as a result of polarization effects. Previously it has been determined that amide-amide hydrogen bonding is strongest when the N-H···O hydrogen angle approaches linearity; see: Peters, D.; Peters, J. *J. Mol. Struct.* **1980**, *68*, 225.
(20) The strain energy of cycloalkanes decreases from 27.5 kcal/mol for cyclopropane to 0.1 kcal/mol for cyclohexane and then increases to a value of 11.1 kcal/mol for cycloundecane after which it decreases again: Skinner, H. A.; Pilcher, G. *Quart. Rev.* **1963**, *17*, 264.
(21) Singelenberg, F. A. J.; Lutz, E. T. G.; van der Maas, J. H. *J. Mol. Struct.* **1991**, *245*, 173.

before.[14] Coupling of the amine terminated monomethyl ethylene oxides **2a**−**2g** with 1′-carbonyldiimidazole activated tridecyl pyrimidinone **3** resulted in the desired oligoEO substituted 2-ureido-pyrimidinones **1a**−**g** (Scheme 1). The synthesis of the amine terminated monomethyl ethylene oxides **2c**, **2d**, **2f** ,and **2g** is reported in the Supporting Information.

SCHEME 1. Synthesis of OligoEO Substituted 2-Ureido-pyrimidinones 1a−g[a]

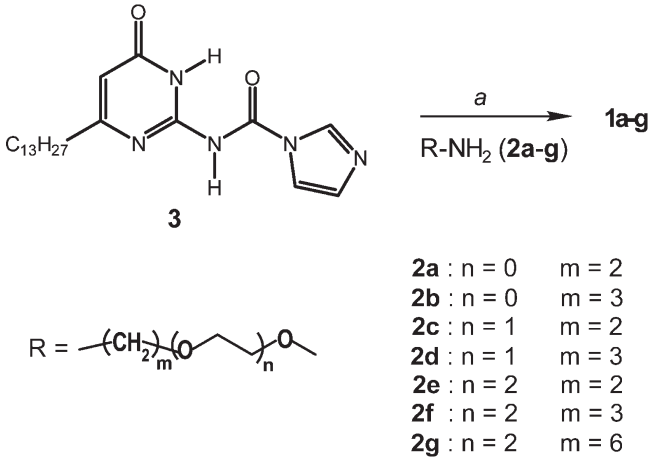

[a]Reagents and conditions for *a*: amine terminated mono-methyl ethylene oxides **2a**−**2g**, $CHCl_3$, 48 h, 60 °C, NEt_3 (for **2g**).

Assessment of Dimerization Strength Using ^{1}H NMR. The dimerization strength of oligoEO substituted 2-ureido-pyrimidinones **1a**−**g** was probed using ^{1}H NMR spectroscopy in anhydrous $CDCl_3$. Previously we reported[14] that upon dilution of tri(ethylene glycol) monomethyl ether substituted UPy **1e** in which the oligoEO chain is connected *via* a C_2 spacer ($m = 2$), an additional signal at δ 5.86 ppm appears in the region of the ^{1}H NMR spectrum where the signals of the alkylidene protons resonate. We have used DOSY NMR to confirm that this signal at δ 5.86 ppm belongs to monomeric 2-ureido-pyrimidinone, whereas the signal at δ 5.82 ppm belongs the quadruple hydrogen-bonded dimer.[14] On the basis of the integral ratio between the monomeric and dimeric signals in the ^{1}H NMR spectrum of **1e** at 25 °C in anhydrous $CDCl_3$, a K_{dim} of $3 \pm 0.2 \times 10^4$ M^{-1} was calculated.[14]

Further examination of the ^{1}H NMR spectrum of UPy **1f**, in which the oligoEO chain is connected *via* a C_3 spacer ($m = 3$), in $CDCl_3$ shows concentration-dependent changes in the region where the inter- and intramolecular hydrogen-bonded NH protons resonate (Figure 1a) as well as in the region where the methylene protons of the oligoEO chain resonate (Figure 1c). For example, the two intermolecular hydrogen-bonded protons of the quadruple hydrogen-bonded UPy dimer **1f·1f** located at 11.96 and 10.3 ppm are shifted upfield to 8.76 and 6.5 ppm in monomeric **1f**. The sharpness and relative downfield position of the two NH protons at 8.76 and 6.5 ppm in monomeric **1f** gives a strong indication that these protons are hydrogen-bonded. On the basis of the integral ratio between the signals belonging to monomeric and dimeric **1f**, a K_{dim} of $7.7 \pm 0.6 \times 10^4$ M^{-1} at 25 °C in anhydrous $CDCl_3$ was calculated.

To exclude the possibility that the lower dimerization constant of UPy dimers **1e·1e** and **1f·1f** is either a result of competitive *inter*molecular hydrogen-bonding or an increase in the polarity of the solution due to attachment of the short tri(ethylene glycol) chain to the UPy unit, ^{1}H NMR dilution experiments in anhydrous $CDCl_3$ were conducted on a 1:1 mixture of di(ethylene glycol) dimethyl ether and an UPy compound (**11**) bearing only aliphatic side chains. The ^{1}H NMR spectrum of this mixture at a concentration of 0.05 mM in $CDCl_3$ clearly shows that **11** is fully dimerized at this concentration as no signals corresponding to the monomer are present (see Supporting Information). Hence, from these experiments it can be concluded that the lowered dimerization constant of UPy dimers **1e·1e** and **1f·1f** is a result of a competitive *intra*molecular effect, presumably intramolecular hydrogen-bonding of the ureido NH protons to the oxygen atoms of the tri(ethylene glycol) chain.

To delineate the relation between the length of the aliphatic spacer (m) and the number of EO units (n), ^{1}H NMR dilution experiments were performed on all UPy compounds **1a**−**g** in anhydrous $CDCl_3$ up to a concentration of 0.5 mM. On the basis of these dilutions the K_{dim} value can be calculated if $K_{dim} < 10^6$ M^{-1} (Table 1).[22] From the data in Table 1 it can be concluded that the value of K_{dim} decreases as the number of EG units (n) is increased and within the series $n = 2$ increases as the total number of carbon atoms (m) between the ureido NH proton and the first oxygen atom of the oligoEO chain is increased from 2 to 6. For a shorter oligoEO chain ($n = 1$) the situation is less straightforward as in this case K_{dim} decreases upon going from $m = 2$ to $m = 3$ (*vide infra*).

TABLE 1. Dimerization Constants for Compounds 1a−g Determined by ^{1}H NMR Dilution Experiments in Anhydrous $CDCl_3$ at 25 °C

compound	K_{dim} (M^{-1})
1a ($n = 0, m = 2$)	$> 10^6$
1b ($n = 0, m = 3$)	$> 10^6$
1c ($n = 1, m = 2$)	$> 10^6$
1d ($n = 1, m = 3$)	$5 \pm 1 \times 10^5$
1e ($n = 2, m = 2$)	$3 \pm 0.5 \times 10^4$
1f ($n = 2, m = 3$)	$7.7 \pm 0.6 \times 10^4$
1g ($n = 2, m = 6$)	$> 10^6$

Infrared Spectroscopy. FT-IR spectroscopy is a powerful tool for the evaluation of the preferred conformation[23] of the terminal oligoEO chains in UPy compounds **1a**−**g**. Previous FT-IR studies on monodisperse oligoEO chains in various solvents have shown that the *anti* and *gauche* conformations of the C−C and C−O bonds have different stretching vibrations.[24] Because backfolding of the oligoEO chain to the acidic NH protons of the UPy motif results in a change of the oligoEO chain from a linear to a bent conformation, it was expected that this process could be conveniently monitored by FT-IR.[14] To minimize the number of C−C bonds, FT-IR dilution experiments in $CDCl_3$ were performed on

(22) Under the assumption that at least 10% dissociation is required to be observable at the final concentration (0.05 mM), a lower limit on the dimerization constant can be placed: $K_{dim} > 1 \times 10^6$ M^{-1}.

(23) (a) Wahab, S. A.; Matsuura, H. *Phys. Chem. Chem. Phys.* **2001**, *3*, 4689. (b) Begum, R.; Yonemitsu, T.; Matsuura, H. *J. Mol. Struct.* **1998**, *447*, 111. (c) Begum, R.; Matsuura, H. *J. Chem. Soc. Faraday Trans.* **1997**, *93*, 3839.

(24) Key bands at 1355−1360 cm^{-1} and 1335−1320 cm^{-1} for the respective *gauche* and *anti* C-C conformations, while those at 1310−1297 cm^{-1} and 1290−1295 cm^{-1} for the *gauche* and *anti* C-O conformations, respectively.

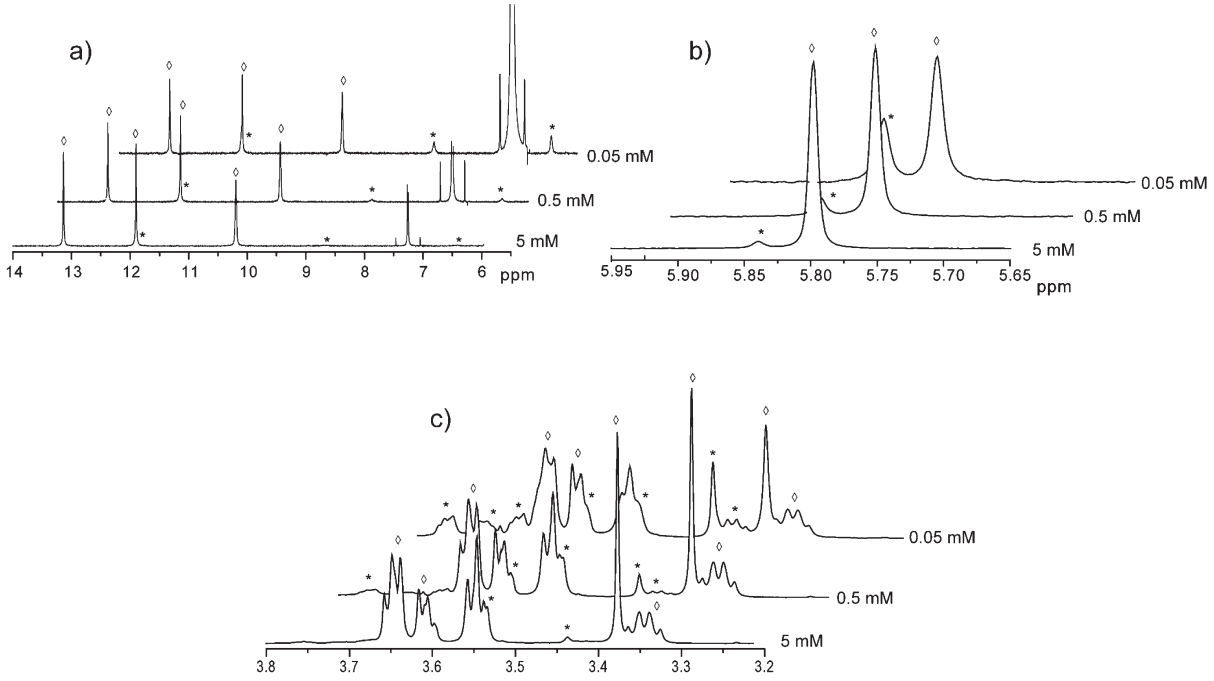

FIGURE 1. Partial ^{1}H NMR spectra of **1f** in $CDCl_3$ (T = 25 °C) at different total concentrations of **1f**, showing (a) changes in the region where the NH protons resonate, (b) changes in the region where the C═CH protons on the ureido-pyrimidinone ring resonate, and (c) the changes in the region where the $NHC\underline{H}_2C\underline{H}_2OC\underline{H}_2C\underline{H}_2OC\underline{H}_2C\underline{H}_2OC\underline{H}_3$ protons resonate. The symbols denote signals belonging to dimeric (◊) and monomeric (∗) species.

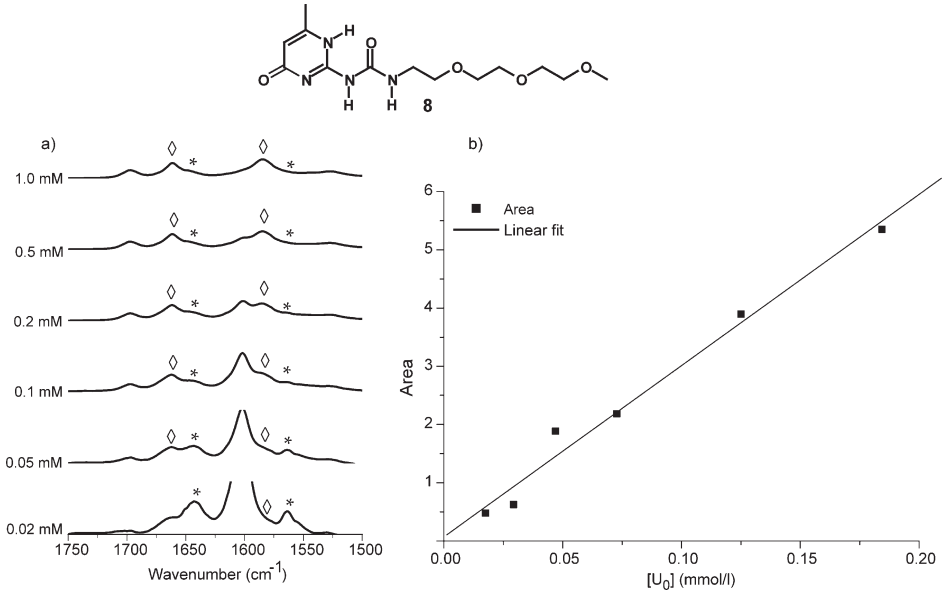

FIGURE 2. FT-IR dilution of **8** in $CDCl_3$ at room temperature. (a) Amide I and amide II region of the FT-IR spectrum of **8** in $CDCl_3$ normalized for the concentration of UPy (U_0). The symbols denote signals belonging to dimeric (◊) and monomeric (∗) species. The band at 1600 cm^{-1} is assigned to residual water in the sample. (b) Relative area of the IR band at 1560 cm^{-1} obtained by deconvolution plotted against the calculated monomer concentration (U_0).

model compound **8** ($m = 2, n = 2$) bearing a methyl group at the C_6 position of the pyrimidinone ring (Figure 2). The dimerization constant of this compound was determined to be 1.2×10^4 M^{-1} based on the integrals of the monomer and dimer in the ^{1}H NMR spectrum obtained at 0.1 and 0.05 mM. Unfortunately, the changes in the region between 1290 and 1360 cm^{-1}, characteristic for the changes in the C−C and C−O stretch vibrations, could not be followed at low concentrations because of the low intensity of the peaks in this region and the presence of artifacts caused by the high concentration of solvent. However, it proved possible to probe the changes in the amide I and amide II region (between 1500 and 1750 cm^{-1}) as a function of concentration due to the higher intensity of the absorptions present in this

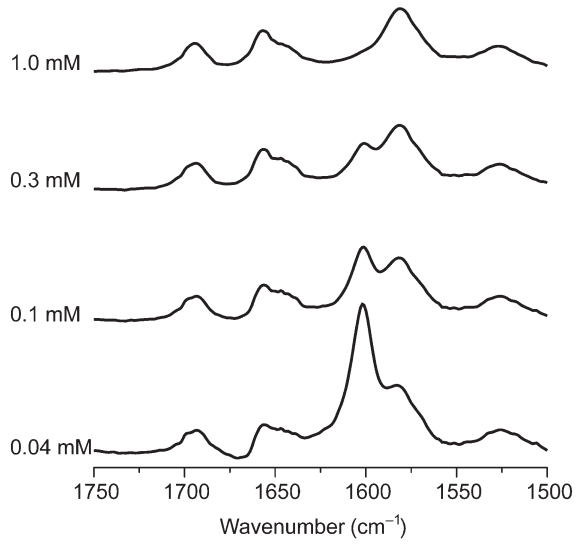

FIGURE 3. Amide I and amide II region of the FT-IR spectrum at various concentrations of **1g** in $CDCl_3$ at room temperature. The band at 1600 cm^{-1} is assigned to residual water in the sample.

region. Concentration-dependent infrared measurements performed on a solution of **8** in $CDCl_3$ revealed significant changes in the amide I and amide II region, indicative of a rearrangement of the hydrogen bond array. As can be observed from Figure 2, the most pronounced changes can be observed in the bands at 1550−1590 cm^{-1} and 1625−1675 cm^{-1}.

To allow for a quantitative analysis, the FT-IR spectrum between 1500 and 1710 cm^{-1} at each concentration was deconvoluted into seven peaks using a Lorentzian[25] line shape (Figure 2b). A plot of the relative area of the band at 1560 cm^{-1} (corrected for the concentration) against the calculated monomer concentration reveals that this band indeed originates from monomeric ureido-pyrimidinone. To further prove the claim that the K_{dim} of **1g** ($m = 6$, $n = 2$) is indeed much higher than that of **8** ($m = 2$, $n = 2$), concentration-dependent FT-IR measurements were also conducted on **1g** in $CDCl_3$. As can be observed from the concentration-dependent FT-IR spectra (Figure 3), no spectral changes on diluting from 1 to 0.04 mM occur, in agreement with the much higher K_{dim} value of **1g** ($> 10^6$ M^{-1}) as found using ^{1}H NMR spectroscopy.

UV−vis Spectroscopy. UV−vis spectroscopy provides a convenient tool to evaluate the tautomeric preference of the pyrimidinone ring.[26] More specifically, it has been shown that the 4[1*H*] pyrimidinone tautomer has an absorption maximum at 260 nm, whereas the 6[1*H*] tautomer has an absorption maximum at 285 nm. Because no experimental data is available for the enol tautomer, a theoretical study on the various monomeric pyrimidinone tautomers using TDDFT (time-dependent DFT) was performed. TDDFT is well-known as a rigorous formalism for the treatment of excitation energies within the DFT framework.[27] The combination of efficiency as well as precision makes TDDFT very attractive, and as a result it has been applied for the calculation of excitation energies of simple molecules[28] and large systems.[29] The TDDFT calculations on 2-ureido-pyrimidinone monomer **9b** and dimers **9a**·**9a** and **9c**·**9c** were performed using the hybrid PBE0 functional[30] in conjunction with the standard 6-311++G(2d,p) triple split basis set[31] using the Gaussian03 suite of programs.[32] The effect of solvent ($CHCl_3$) on the excitation energies was taken into account using the polarizable continuum model (PCM) of nonequilibrium solutions.[33]

As can be observed from the calculated oscillator strengths of the three different tautomeric forms (Figure 4a), the 6[1*H*] tautomer has an absorption at high wavelengths that is not present in the two other tautomeric forms. Figure 4b shows the measured UV−vis spectra of 0.05 mM solutions of **1a**−**f** in $CHCl_3$. The extinction coefficient at 285 nm, corresponding to the 6[1*H*] tautomer, is largest for the compounds with the lowest K_{dim}, indicating that the fraction present as the 6[1*H*] monomeric form is the largest for these. Moreover, the values of the extinction coefficient follow the order of K_{dim} as determined by the ^{1}H NMR experiments (Table 1).

^{1}H NMR Coupling Constant Analysis. To gain more insight into the cause of the reduced K_{dim} of UPy compounds **1e** and **1f** ($n = 2$), a 2D NOESY experiment was conducted on a 0.5 mM solution of **1f** in $CDCl_3$. Molecular models of **1f** in the *transoid*,*transoid* 6[1*H*] tautomeric form indicate that the distance between the ureido-NH protons and the closest methylene protons of the EO chain should be within 4 Å when the polyether oxygen atoms are hydrogen-bonded to the NH protons of the urea functionality. Unfortunately, no NOE between these protons could be observed at a concentration of 0.5 mM in $CDCl_3$, most possibly due to the low fraction of the 6[1*H*] tautomer at this concentration. 2D NOESY experiments conducted at lower concentration also failed as a result of the low signal-to-noise ratio due to the low sensitivity of the 2D NOESY sequence.

(25) Meier, R. J. *Vib. Spectrosc.* **2005**, *39*, 266.

(26) (a) Morita, H.; Nagakura, S. *Theor. Chim. Acta* (*Berlin*) **1968**, *11*, 279. (b) Brown, D. J.; Teitei, T. *Aus. J. Chem.* **1965**, *18*, 559.

(27) (a) Gross, E. K. U.; Kohn, W. *Adv. Quant. Chem.* **1990**, *21*, 255. (b) Gross, E. K. U.; Dobson, J. F.; Petersilka, M. In *Density Functional Theory*; Nalewajski, R. F., Ed.; Springer Series "Topics in Current Chemistry"; Springer: Heidelberg, 1996; Vol. 81, p 81. (c) Jamorski, C.; Casida, M. E.; Salahub, D. R. *J. Chem. Phys.* **1996**, *104*, 5134.

(28) (a) Improta, R.; Barone, V.; Santoro, F. *Angew. Chem., Int. Ed.* **2007**, *46*, 405. (b) Santoro, F.; Barone, V.; Benzi, C.; Improta, R. *Theor. Chem. Acc.* **2007**, *117*, 1073. (c) Jacquemin, D.; Perpète, E. A.; Scuseria, G. E.; Ciofini, I.; Adamo, C. *J. Chem. Theory Comput.* **2008**, *4*, 123.

(29) (a) Jödicke, C. J.; Lüthi, H. P. *J. Am. Chem. Soc.* **2003**, *125*, 252. (b) Santoro, F.; Barone, V.; Improta, R. *Proc. Natl. Acad. Sci. U.S.A.* **2007**, *104*, 9931. (c) van Gisbergen, S. J. A.; Schipper, P. R. T.; Gritsenko, O. V.; Baerends, E. J.; Snijders, J. G.; Champagne, B.; Kistman, B. *Phys. Rev. Lett.* **1999**, *83*, 694. (d) Bauernschmitt, R.; Ahlrichs, R.; Hennrich, F. H.; Kappes, M. M. *J. Am. Chem. Soc.* **1998**, *120*, 5052.

(30) (a) Adamo, C.; Barone, V. *J. Chem. Phys.* **1999**, *110*, 6158. (b) Perdew, J. P.; Burke, K.; Ernzerhof, M. *Phys. Rev. Lett.* **1996**, *77*, 3865.

(31) The 6-311G++(2d,p) triple valence basis set was selected due to it is good performance in a number of other TDDFT studies. See ref 28c and references therein.

(32) Frisch, M. J.; Trucks, G. W.; Schlegel, H. B.; Scuseria, G. E.; Robb, M. A.; Cheeseman, J. R.; Zakrzewski, V. G.; Montgomery, J. A., Jr.; Stratmann, R. E.; Burant, J. C.; Dapprich, S.; Millam, J. M.; Daniels, A. D.; Kudin, K. N.; Strain, M. C.; Farkas, O.; Tomasi, J.; Barone, V.; Cossi, M.; Cammi, R.; Mennucci, B.; Pomelli, C.; Adamo, C.; Clifford, S.; Ochterski, J.; Petersson, G. A.; Ayala, P. Y.; Cui, Q.; Morokuma, K.; Malick, D. K.; Rabuck, A. D.; Raghavachari, K.; Foresman, J. B.; Cioslowski, J.; Ortiz, J. V.; Stefanov, B. B.; Liu, G.; Liashenko, A.; Piskorz, P.; Komaromi, I.; Gomperts, R.; Martin, R. L.; Fox, D. J.; Keith, T.; Al-Laham, M. A.; Peng, C. Y.; Nanayakkara, A.; Gonzalez, C.; Challacombe, M.; Gill, P. M. W.; Johnson, B. G.; Chen, W.; Wong, M. W.; Andres, J. L.; Head-Gordon, M.; Replogle, E. S.; Pople, J. A. *Gaussian 03, Revision B.04*; Gaussian, Inc.: Wallingford CT, 2003.

(33) (a) Cossi, M.; Barone, V. *J. Phys. Chem. A* **2000**, *104*, 10614. (b) Aguilar, M. A. *J. Phys. Chem. A* **2001**, *105*, 10393.

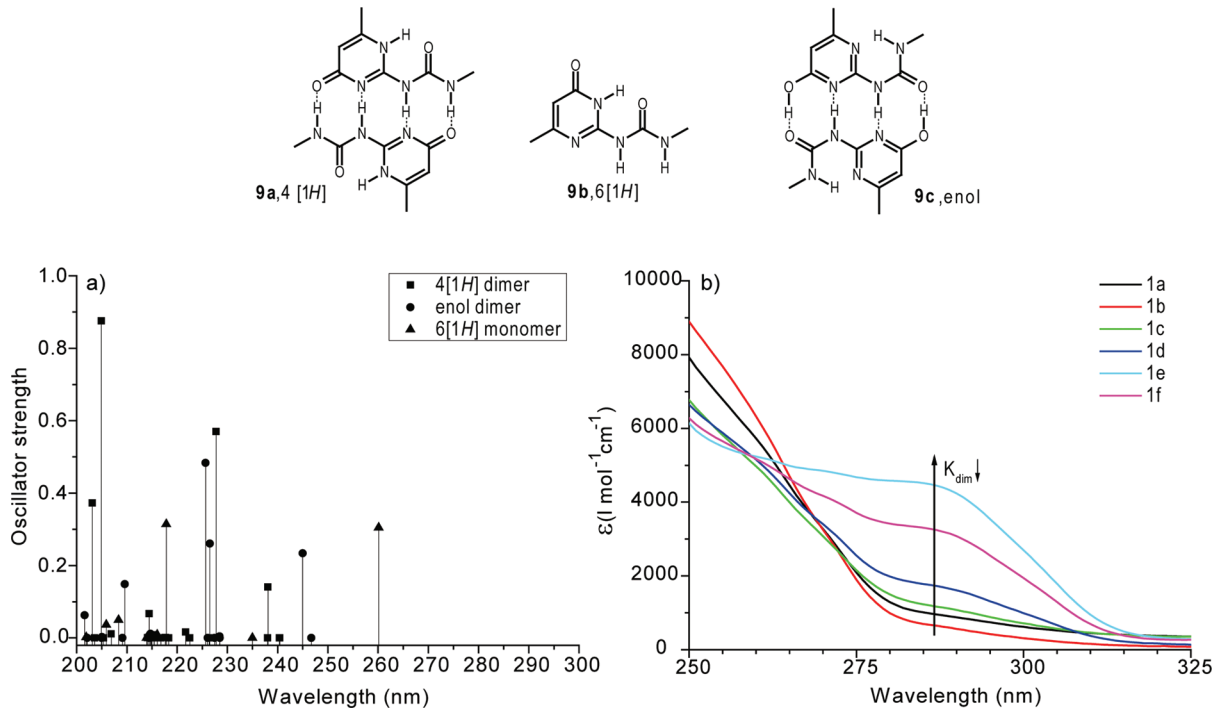

FIGURE 4. (a) Calculated oscillator strength stick spectra of 2-ureido-pyrimidinone tautomers **9a**−**c** at 0 K. (b) Partial UV−vis spectra of 0.05 mM solutions of compounds **1a**−**f** in $CHCl_3$ (T = 25 °C).

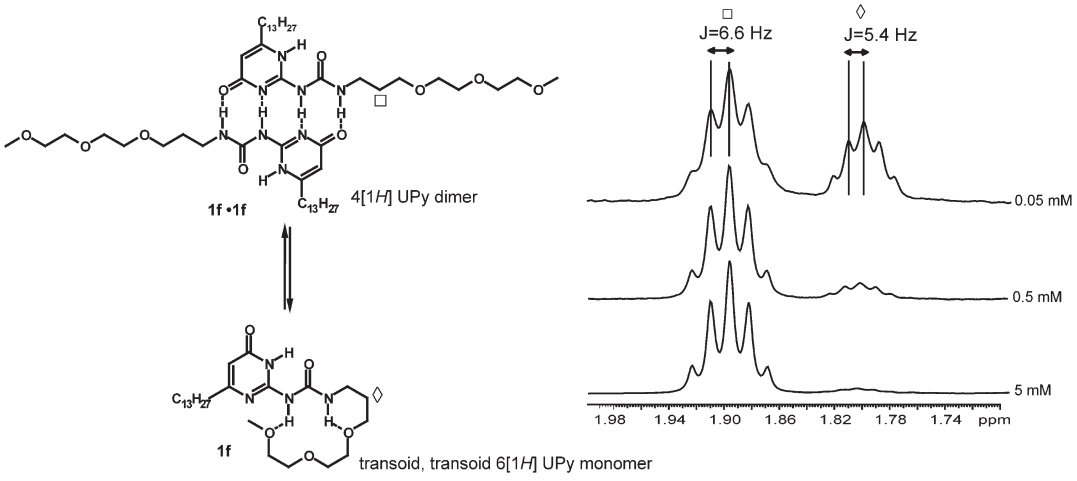

FIGURE 5. (Right) Partial ^{1}H NMR spectrum of UPy **1f** in $CDCl_3$ (T = 25 °C) showing the splitting pattern of the central methylene protons of the C_3 spacer. (Left) Display of the conformational changes in the C_3 spacer upon going from the 4[1*H*] UPy dimer to the 6[1*H*] UPy monomer, the latter in which the oligoEO chain is hydrogen-bonded to the ureido NH protons.

^{1}H NMR coupling constant analysis is a common technique for the evaluation of conformational equilibria in molecules. The relation between the $^3J_{HH}$ coupling constant and the dihedral torsion angle was first described by Karplus[34] and later generalized by Haasnoot and Altona.[35] In general, the coupling constants are largest for dihedral angles close to 180° (*anti* conformation). As previously mentioned, two sets of signals, corresponding to the 4[1*H*] UPy dimer and the 6[1*H*] UPy monomer, are visible at low concentrations of **1f** in $CDCl_3$. Unfortunately, ^{1}H NMR coupling constant analysis on the -O-C$\underline{H}_2$-C$\underline{H}_2$-O- protons could not be performed because of the overlapping sets of peaks originating from UPy monomer and dimer in the region between 3 and 3.8 ppm. However, ^{1}H NMR coupling constant analysis of the central methylene protons in the C_3 spacer of **1f** revealed that the two multiplets have different coupling constants, i.e., 6.6 Hz for the dimer and 5.4 Hz for the monomer (Figure 5). The decrease of the coupling constant can be explained by an increase in the fraction of C−C bonds adopting a *gauche* conformation in the C_3 spacer of the monomer compared to the C_3 spacer of its dimer (Figure 5). This strongly indicates that the C_3 chain connecting the oligoEO chain with the 2-ureido-pyrimidinone

(34) (a) Karplus, M. *J. Chem. Phys.* **1959**, *80*, 11. (b) Karplus, M. *J. Am. Chem. Soc.* **1963**, *85*, 2870.
(35) Haasnoot, C. A. G.; De Leeuw, F. A. A. M.; Altona, C. *Tetrahedron* **1980**, *36*, 2783.

TABLE 2. UPy Dimerization Constant and UPy·NaPy Association Constant of UPy 1e, 1f, and 1g and NaPy 10 in $CDCl_3$ (K_{dim}) and $CHCl_3$ (K_a) at 25 °C

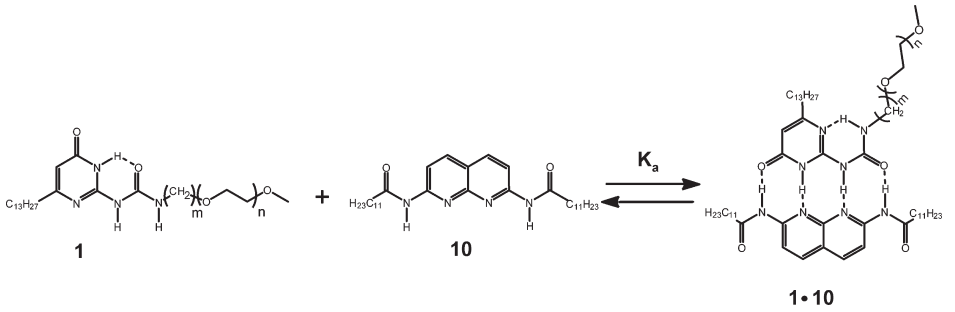

compound	K_{dim} (M^{-1})	K_a (M^{-1})
1e	$3 \pm 0.5 \times 10^4$	$9.6 \pm 0.2 \times 10^4$
1f	$7.7 \pm 0.6 \times 10^4$	$6.9 \pm 0.4 \times 10^4$
1g	$> 10^6$	$0.55-3.5 \times 10^6$

unit undergoes a conformational change as the UPy tautomerizes from the 4[1*H*] dimer to the 6[1*H*] monomer, in agreement with our backfolding hypothesis.

Heterodimer Formation of TriEO Substituted Ureido-pyrimidinones with 2,7-Diamido-1,8-naphthyridine. Besides homodimer formation, the UPy unit is also able to selectively form strong heterodimers with 2,7-diamido-1,8-naphthyridine (NaPy) when UPy is in the *cisoid*,*transoid* 6[1*H*] tautomeric form as it presents a hydrogen-bonding acceptor-donor-donor-acceptor (ADDA) array.[36] As shown by Zimmerman and us, the fidelity of UPy·NaPy heterodimer formation is greatly increased if the UPy dimerization constant (K_{dim}) is much lower than the association constant (K_a) of the UPy·NaPy heterodimer.[37]

To gain insight into the effect of short oligoEO chains on the association constant of the UPy·NaPy heterocomplex, UV−vis titrations in $CHCl_3$ and subsequent analysis of the titration curves with a previously reported modified[38] 1:1 binding model were performed. Because the K_{dim} of **1e** and **1f** is precisely known, the K_a of **1e** and **1f** with NaPy **10** could be reliably obtained by UV−vis titrations. As is shown in Table 2, the K_a values of **1e** ($m = 2, n = 2$) and **1f** ($m = 3, n = 2$) with **10** are 50−80 times lower compared to the value of K_a of **10** with 2-ureido-pyrimidinone substituted with an aliphatic substituent ($K_a \approx 5 \times 10^6$ M^{-1} in $CHCl_3$).[38]

Given the fact that the K_{dim} of UPy **1g** ($m = 6$, $n = 2$) could not precisely be determined, the absorption data obtained from the titration of **1g** and **10** was analyzed with two different values of K_{dim} corresponding to the lowest (10^6 M^{-1}) and highest (6×10^7 M^{-1}) estimate of K_{dim}. In this way, the value of K_a of **1g·10** was determined to be in the range of $0.55-3.5 \times 10^6$ M^{-1} in $CHCl_3$, which is close to the value of 5×10^6 M^{-1} found for 2-ureido-pyrimidinone dimers substituted with aliphatic substituents.[38] From this data it is concluded that substitution of triEO chains ($n = 2$) to UPy dimers results in a reduction of binding strength with 2,7-diamido-1,8-naphthyridine when short spacers are used to connect the triEO chain to the urea functionality of the UPy unit.

Discussion. The results from the UV−vis studies clearly show that the UPy compounds displaying a reduced K_{dim} are present in their 6[1*H*] tautomeric form at low concentrations. Moreover, the FT-IR experiments show a rearrangement of the hydrogen bonding array, as is evident by the large concentration-dependent changes in the amide I and amide II region of the spectrum. Finally, although a NOE between the ureido NH and the methylene groups of the EO chain could not be detected, analysis of the coupling constant of the central CH_2 protons of the C_3 spacer in UPy compound **1f** did show evidence of backfolding of the oligoEO chain in the monomeric form of **1f**.

Taking all of the results into account, two mechanisms can be thought to be responsible for the reduction of K_{dim} in oligoEO substituted 2-ureido-pyrimidinones: (1) Hydrogen bonding of the ether oxygen atoms of the oligoEO chain to the acidic NH protons of the urea in the *transoid*,*transoid* 6[1*H*] UPy monomeric form, causing an additional stabilization of this tautomer compared to the dimerizing 4[1*H*] tautomer. Because the experimentally determined K_{dim} is the product of the tautomerization constant squared (K_{taut}, defined as K_{taut} = concentration 4[1*H*] monomer/concentration 6[1*H*] monomer) and the true dimerization constant of the 4[1*H*] monomer (K_{dim}* defined as concentration 4[1*H*] dimer/(concentration 4[1*H*] monomer)^2), it can be easily recognized that an increase in the stability of the 6[1*H*] tautomer leads to a rapid decrease in the observed K_{dim} (Figure 6a) due to a decrease in K_{taut}. As was explained previously, the stabilizing effect of intramolecular hydrogen bonding of the oligoEO chain on the 6[1*H*] monomer will be lower for longer spacers (increasing *m*) as a result of entropic effects, whereas it will increase with the number of possible interactions (*n*). (2) Repulsive electrostatic interactions

(36) (a) Corbin, P. S.; Zimmerman, S. C. *J. Am. Chem. Soc.* **1998**, *120*, 9710. (b) Wang, X.-Z.; Li, X.-Q. ; Shao, X.-B.; Zhao, X.; Deng, P.; Jiang, X.-K.; Li, Z.-T.; Chen, Y.-Q. *Chemistry* **2003**, *9*, 2904. (c) Ligthart, G. B. W. L.; Ohkawa, H.; Sijbesma, R. P.; Meijer, E. W. *J. Am. Chem. Soc.* **2005**, *127*, 810.

(37) (a) Todd, E. M.; Quinn, J. R.; Park, T.; Zimmerman, S. C. *Isr. J. Chem.* **2005**, *45*, 381. (b) de Greef, T. F. A.; Ercolani, G.; Ligthart, G. B. W. L.; Meijer, E. W.; Sijbesma, R. P. *J. Am. Chem. Soc.* **2008**, *130*, 13755.

(38) Previously, we have shown that the association constant of the quadruple hydrogen-bonded complex of 2-ureido-pyrdiminone with 2,7-diamido-1,8-naphthyridine can be obtained by spectrophotometric titrations. Upon addition of UPy to a solution of NaPy in $CHCl_3$ the absorption intensity at 355 nm increases. The absorbance at 355 nm as a function of added UPy can be analyzed with a 1:1 binding model accompanied by dimerization of one of the components. See: de Greef, T. F. A.; Ligthart, G. B. W. L.; Lutz, M.; Spek, A. L.; Meijer, E. W.; Sijbesma, R. P. *J. Am. Chem. Soc.* **2008**, *130*, 5479.

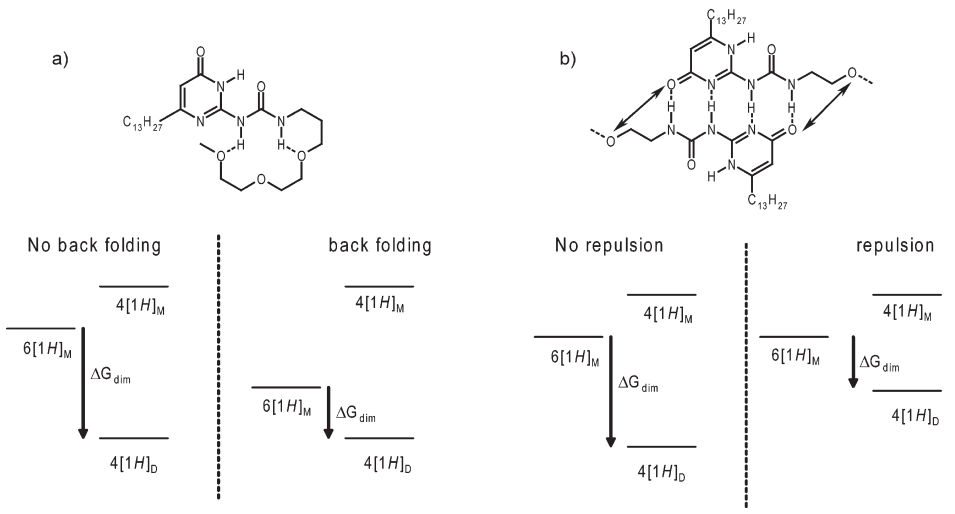

FIGURE 6. Effect of short oligoEO chains on the thermodynamics of UPy dimerization. (a) Effect of stabilization of the 6[1*H*] tautomer, resulting in a reduction in K_{dim} (and hence ΔG_{dim}). (b) Effect of repulsive electrostatic interactions, resulting in destabilization of the 4[1*H*] dimer and subsequent reduction in K_{dim}. The subscripts M and D denote monomer and dimer, respectively.

between the first oxygen of the oligoEO chain and the carbonyl group of the pyrimidinone ring (Figure 6b). In this case the K_{dim} is lowered because the UPy 4[1*H*] dimer is destabilized with respect to its aliphatic counterpart. For this interaction, the largest effect on K_{dim} is expected for the shortest spacer (small *m*).

As can be observed from Table 1 and Figure 4b, within the series $n = 2$, K_{dim} increases as *m* is increased. As the oligoEO chain for $n = 2$ is large enough to form intramolecular hydrogen bonds to both NH protons, this increase in K_{dim} as *m* grows larger is a direct result of an increasing entropic penalty for cyclization for larger aliphatic spacers. Furthermore, the number of unfavorable *gauche* interactions, induced in the aliphatic spacer as it bends back upon itself, also increases as *m* grows larger resulting in a higher enthalpic offset for back folding of the larger spacers. In addition to these effects, the effect of repulsive electrostatic interactions is the highest for $m = 2$.

As already noted, within the series $n = 1$, the opposite behavior is observed, i.e., upon increasing *m* from 2 to 3, K_{dim} decreases. To understand the cause of this effect, Monte Carlo conformational searching using the OPLS 2005 force field and the GB/SA solvation model ($CHCl_3$) was performed using Macromodel 9.5 on derivatives of **1c** and **1d** in which the tridecyl chain is substituted for a methyl group. Subsequently, the lowest energy conformers of **1c** and **1d** found using this procedure were optimized at the B3LYP//6-311G+(d,p)//PCM($CHCl_3$) level of theory. Analysis of the hydrogen bond geometries of both conformers show that in the case of **1d** ($m = 3$) the hydrogen bond lengths are between 1.91 and 2.16 Å, while the N−H···O angles are 138° and 172°, respectively. On the other hand, the hydrogen bond lengths in the folded conformation of **1c** ($m = 2$) are much larger, i.e., between 1.93 and 2.52 Å, while the angles are 163° and 141°, respectively (Figure 7). Statistical surveys of crystallographic data suggest that the optimum bond distances are approximately 1.9 Å for H···O and that hydrogen bonding is strongest when the NH···O angle

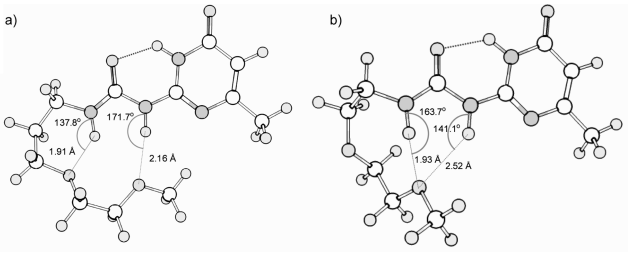

FIGURE 7. Energy minimized structures (DFT, B3LYP//6-311G+(d,p)//PCM($CHCl_3$)) of (a) *transoid*,*transoid* 2-ureido-6[1*H*]-pyrimidinone **1d** ($m = 3$, $n = 1$) and (b) *transoid*,*transoid* 2-ureido-6[1*H*]-pyrimidinone **1c** ($m = 2$, $n = 1$). Note that the aliphatic tridecyl chain in **1c** and **1d** has been replaced by a CH_3 group to reduce calculation time.

approaches linearity.[19,39,40] Taking into account these findings and the calculated hydrogen bond lengths and angles in the lowest energy conformers of **1c** and **1d**, it can be concluded that the extent of intramolecular hydrogen bonding is much higher in monomeric **1d** compared to **1c** as a result of the fact that the longer aliphatic spacer in **1d** allows simultaneous binding of both NH protons to the ether oxygen atoms of the oligoEO chain.

Furthermore, the calculations reveal that the oligoEO chain of **1d** can form multiple hydrogen bonds without violating stereochemical restrictions, i.e., all torsion angles C-C-O-C and C-O-C-C along the polyether chain are *anti* (between 162° and 178°), while the O-C-C-O torsion angles are *gauche* (60°), as is also observed in the crystal structure of a 1:1 complex of urea and bis[2-*o*-methoxyphenoxy]ethyl] ether.[41] Although the presented analysis only takes into account the hydrogen bond geometry in the lowest energy conformers of **1c** and **1d**, similar effects are also expected in other conformers in which the conformation of the oligoEO chain is different. More importantly, the higher dimerization constant of UPy **1c** compared to that of UPy **1d** is a clear indication that an increase in microenvironment polarity

(39) Baker, E. N.; Hubbard, R. E. *Prog. Biophys. Mol. Biol.* **1984**, *44*, 97.

(40) Mitchell, J. B. O.; Price, S. L. *Chem. Phys. Lett.* **1989**, *154*, 267.

(41) Chacko, K. K.; Narasimhan, P. *Acta Crystallogr.* **1984**, *C40*, 160.

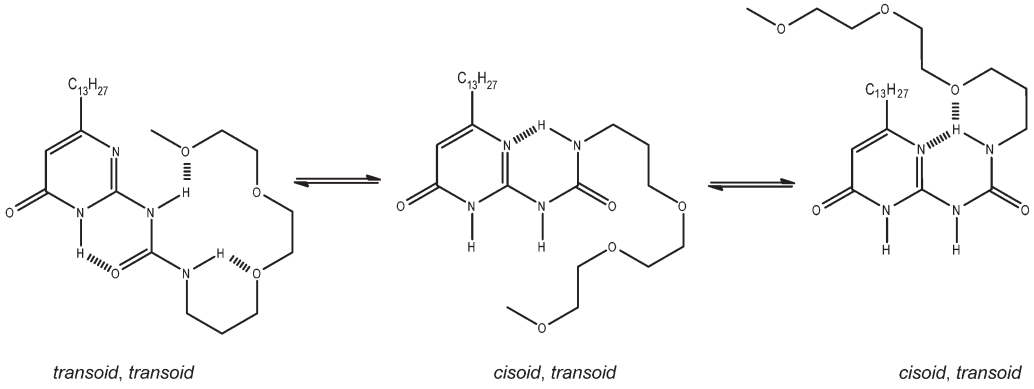

FIGURE 8. Conformational equilibria of the 2-ureido-6[1*H*]-pyrimidinone tautomers of **1f**. Backfolding of the oligoEO chains is geometrically more feasible in the *transoid*,*transoid* conformer.

created by the polar oligoEO chain is not the main driving force for the decrease in the dimerization constant of EO substituted 2-ureido-pyrimidinones, as the UPy with the longer and more apolar spacer (**1d**) displays the largest reduction in dimerization strength.

In comparison to the association constant (K_a) that has been reported for 2-ureido-pyrimidinones carrying aliphatic chains, the K_a of oligoEO substituted 2-ureido-pyrimidinones with 2,7-diamido-1,8-naphthyridine is reduced by roughly 2 orders of magnitude. This reduction can also be attributed to backfolding. As explained previously, the *cisoid*,*transoid* 6[1*H*] tautomeric form of UPy can bind to 2,7-diamido-1,8-naphthyridine resulting in the formation of an ADDA quadruple hydrogen-bonded array. However, stabilization of this conformer by intramolecular hydrogen bonding of the ether oxygen atoms present in the oligoEO chain is much less favorable compared to intramolecular hydrogen bonding of the oligoEO chain in the *transoid*, *transoid* conformer (Figure 8). Hence, also in this case stabilization, of the *transoid*,*transoid* 6[1*H*] monomer results in a perturbation of the equilibrium ultimately resulting in a decrease of K_a. It is interesting to note that although UPy dimerization is lowered by a factor of 800 for **1f**, the K_a of **1f·10** is only reduced by a factor of 70. The cause of this difference can be 3-fold. First, backfolding of the oligoEO chain to the intramolecular hydrogen bond of UPy **1f** (Figure 8) in the UPy·NaPy complex **1f·10** can cause an increased stabilization of this complex. Second, repulsive electrostatic interactions between the oxygen atoms of the oligoEO chain and the electronegative atoms constituting the hydrogen bond array are much less pronounced in the UPy·NaPy complex compared to the UPy·UPy complex. Finally, while the UPy dimer has two oligoEO chains capable of backfolding, the UPy·NaPy heterodimer has only a single oligoEO chain capable of competing with the formation of the quadruple hydrogen bond array.

As has been shown in this paper, substitution of hydrogen bond directed supramolecular assemblies of UPy·UPy homodimers and UPy·NaPy heterodimers with oligo(ethylene oxide) chains leads to a reduction of hydrogen bond strength in chloroform. The reduction in hydrogen bond strength is strongly dependent on the number of ethylene oxide units in the oligoEO chain and length of the aliphatic spacer connecting the hydrogen bonds of the UPy unit with the oligoEO chain. By analyzing a series of UPy monomers that differ in both the length of this aliphatic spacer and the number of ethylene oxide units in the oligoEO side chain, we find strong evidence that the reduction of hydrogen bond strength is caused by hydrogen-bond-induced backfolding of the ureido NH protons to the oxygen atoms in the oligoEO chain. Although in this paper only UPy based assemblies were reported, it was recently found that substitution of a single alkyl chain with an oligoEO chain severely reduces the association constant of the hydrogen-bond-induced supramolecular polymerization of *N*,*N*′,*N*″-trialkyl-benzene-1,3,5-tricarboxamides in apolar solvents.[14,42] Furthermore, it was found that substitution of the alkyl chains for oligoEO chains resulted in the loss of columnar packing in these compounds in the solid state.[42]

Conclusion. The results described in this paper illustrate the extreme sensitivity of noncovalent assemblies toward substitution with polar groups. As has been noted in the Introduction, oligoEO chains are commonly used in various applications to increase the solubility of compounds in water.[43] However, in almost all cases the influence of the oligoEO chain on the binding properties of the conjugate is not compared to the properties of the unfunctionalized analogue. Although the effects of oligoEO chains on noncovalent interactions in apolar solvents are relatively easy to understand, the situation in water is considerably more difficult as a result of additional hydrogen bonding of water with the oligoEO chain. Recent experiments aiming to elaborate the effect of protein PEGylation have shown that substitution of proteins with PEG chains can result in a decrease in binding affinity due to intramolecular interactions between the PEG chain and the active site of the protein.[44] These results seems to suggest that backfolding of oligo and polyEO chains can also occur in water, especially when electrostatic interactions are involved.

(42) Stals, P. J. M.; Haveman, J. F.; Martín-Rapún, R.; Fitié, C. F. C.; Palmans, A. R. A.; Meijer, E. W. *J. Mater. Chem.* **2009**, *19*, 124.

(43) For example, PEG chains are commonly used to study supramolecular assemblies in water. See: (a) Oshovsky, G. V.; Reinhoudt, D. N.; Verboom, W. V. *Angew. Chem., Int. Ed.* **2007**, *46*, 2366. (b) Ryu, J.-H.; Hong, D.-J.; Lee, M. *Chem. Commun.* **2008**, 1043. (c) Rehm, T.; Schmuck, C. *Chem. Commun.* **2008**, 801.

(44) (a) Kubetzko, S.; Sarkar, C. A.; Plückthun, A. *Mol. Pharmacol.* **2005**, *68*, 1439. (b) Kubetzko, S.; Balic, E.; Waibel, R.; Zangemeister-Wittke, U.; Plückthun, A. *J. Biol. Chem.* **2006**, *281*, 35186. (c) Das, R.; Baird, E.; Allen, S.; Baird, B.; Holowka, D.; Goldstein, B. *Biochemistry* **2008**, *47*, 1017. (d) Hu, T.; Li, D.; Manjula, B. N.; Brenowitz, M.; Prabhakaran, M.; Acharya, S. A. *Biochemistry* **2009**, *48*, 608.

Currently, we are investigating the influence of other side chains containing hydrogen bond acceptors and donors on the UPy dimerization strength to show the generality of the results as displayed in this paper.

Experimental Section

Synthesis of 2-(2-Methoxyethyl)-ureido-6-tridecyl-4[1*H*]pyrimidinone (1a). Activated pyrimidinone **3** (1.94 g, 5.00 mmol) and 2-methoxyethyl amine **2a** (0.75 g, 10.00 mmol) were added to dry $CHCl_3$ (16 mL) and stirred at 60 °C for 2 days. After cooling to room temperature, 50 mL of $CHCl_3$ was added, and the mixture was extracted 3 times with 15 mL of aqueous 1 M HCl, neutralized with 20 mL of saturated $NaHCO_3$ (aq), and washed with 20 mL of brine. After drying with $MgSO_4$ the solvent was removed by evaporation *in vacuo*, resulting in the crude ureido-pyrimidinone (1.66 g, 4.2 mmol). Further purification by silica filtration using 4% methanol in $CHCl_3$ as eluent resulted in pure **1a** as a white powder (1.40 g, 3.5 mmol), mp 118.5−119.8 °C. Yield: 71%. ^{1}H NMR ($CDCl_3$): δ 13.09 (s, 1H, NH), 11.95 (s, 1H NH), 10.33 (s, 1H, NH), 5.82 (s, 1H, O=C-CH=C-CH_2), 3.56 (m, 2H, NH-CH_2-CH_2-O), 3.48 (t, 2H, m, 2H, NH-CH_2-CH_2-O), 3.38 (s, 3H, O-CH_3), 2.45 (t, 2H, CH=C-CH_2-CH_2), 1.62 (m, 2H, CH=C-CH_2-CH_2-CH_2), 1.31−1.25 (m, 20H, -CH_2-), 0.87 (t, 3H, -CH_3). ^{13}C NMR ($CDCl_3$): δ 173.1, 156.9, 154.6, 152.4, 105.9, 71.0, 58.8, 39.6, 32.7, 31.9, 29.6−28.8 (multiple signals), 27.0, 22.7, 14.1. IR (ATR): ν = 2953, 2918, 2850, 1698, 1660, 1582, 1524, 1467, 1438, 1310, 1258, 1212, 1199, 1137, 1124, 1088, 965, 943, 884, 810, 771, 743, 721 cm^{-1}. MALDI-TOF-MS (*m*/*z*): calcd 394.29, obsd 395.26 (MH^+), 417.24 (MNa^+). Anal. Calcd for $C_{21}H_{38}N_4O_3$: C 63.93, H 9.71, N 14.20. Found: C 64.12, H 9.94, N 14.45.

Synthesis of 2-(3-Methoxypropyl)-ureido-6-tridecyl-4[1*H*]pyrimidinone (1b). Activated pyrimidinone **3** (1.94 g, 5.00 mmol) and 3-methoxypropyl amine **2b** (0.89 g, 10.00 mmol) were added to dry $CHCl_3$ (16 mL) and stirred at 60 °C for 2 days. After cooling to room temperature, 50 mL of $CHCl_3$ was added, and the mixture was extracted 3 times with 15 mL of 1 M aqueous HCl, neutralized with 20 mL of saturated $NaHCO_3$ (aq), and washed with 20 mL of brine. After drying with $MgSO_4$ the solvent was removed by evaporation *in vacuo*, resulting in the crude ureidopyrimidinone (1.90 g, 4.65 mmol). Further purification by silica filtration using 4% methanol in $CHCl_3$ as eluent resulted in the pure product as a white powder (1.61 g, 3.95 mmol), mp 89.3−89.9 °C. Yield: 79%. ^{1}H NMR ($CDCl_3$): δ 13.15 (s, 1H, NH), 11.91 (s, 1H, NH), 10.22 (s, 1H, NH), 5.81 (s, 1H, O=C-CH=C-CH_2), 3.45 (t, 2H, CH_2-CH_2-O), 3.35−3.32 (m, 5H, NH-CH_2-CH_2 and O-CH_3), 2.45 (t, 2H, CH=C-CH_2-CH_2), 1.88 (m, 2H, NH-CH_2-CH_2-CH_2-O), 1.62 (m, 2H, CH=C-CH_2-CH_2-CH_2), 1.31−1.25 (m, 20H, -CH_2-), 0.87 (t, 3H, -CH_3). ^{13}C NMR ($CDCl_3$): δ 173.1, 156.7, 154.7, 152.4, 105.8, 70.1, 58.6, 37.0, 32.7, 31.9, 29.6−28.8 (multiple signals), 27.0, 22.6, 14.1. IR (ATR): ν = 2918, 2850, 1698, 1657, 1579, 1524, 1467, 1445, 1395, 1307, 1255, 1212, 1196, 1126, 1109, 946, 884, 813, 792, 771, 741, 722 cm^{-1}. MALDI-TOF-MS (*m*/*z*): calcd 408.31, obsd 409.42 (MH^+), 431.40 (MNa^+). Anal. Calcd for $C_{22}H_{40}N_4O_3$: C 64.67, H 9.87, N 13.71. Found: C 65.10, H 9.97, N 13.85.

Synthesis of 2-[2-(2-Methoxyethoxy)ethyl]ureido-6-tridecyl-4-[1*H*]pyrimidinone (1c). Activated pyrimidinone **3** (0.428 g, 1.1 mmol) and 2-(2-methoxyethoxy)ethyl amine **2c** (0.20 g, 1.6 mmol) were added to dry $CHCl_3$ (4 mL) and stirred at 60 °C for 2 days. After cooling to room temperature, 50 mL of $CHCl_3$ was added, and the mixture was extracted 3 times with 15 mL of 1 M aqueous HCl, neutralized with 20 mL of saturated $NaHCO_3$ (aq), and washed with 20 mL of brine. After drying with $MgSO_4$ the solvent was removed by evaporation *in vacuo*, resulting in the crude ureidopyrimidinone (0.44 g, 1.0 mmol). Further purification by recrystallization from 2-propanol, resulted in pure **1c** as a white powder (0.37 g, 0.85 mmol), mp 92.7−93.1 °C. Yield: 78%. ^{1}H NMR ($CDCl_3$): δ 13.08 (s, 1H, NH), 11.94 (s, 1H, NH), 10.27 (s, 1H, NH), 5.80 (s, 1H, O=C-CH=C-CH_2), 3.67−3.64 (m, 4H, O-CH_2-), 3.54 (m, 2H, O-CH_2-), 3.47 (m, 2H, NH-CH_2-CH_2-O), 3.37 (s, 3H, O-CH_3), 2.45 (t, 2H, CH=C-CH_2-CH_2), 1.62 (m, 2H, CH=C-CH_2-CH_2-CH_2), 1.32−1.26 (m, 20H, -CH_2-), 0.88 (t, 3H, -CH_3). ^{13}C NMR ($CDCl_3$): δ 173.0, 156.8, 154.6, 152.4, 105.8, 72.0, 70.5, 70.3, 69.4, 59.0, 39.5, 32.7, 31.9, 29.6−28.8 (multiple signals), 27.0, 22.7, 14.1. IR (ATR): ν = 2919, 2852, 1698, 1664, 1620, 1585, 1563, 1527, 1489, 1468, 1456, 1398, 1332, 1302, 1261, 1202, 1124, 1029, 983, 947, 884, 854, 808, 771, 744, 722 cm^{-1}. MALDI-TOF-MS (*m*/*z*): 438.32, obsd 439.37 (MH^+), 461.62 (MNa^+). Anal. Calcd for $C_{23}H_{42}N_4O_4$: C 62.98, H 9.65, N 12.77. Found: C 62.87, H 9.79, N 12.76.

Synthesis of 2-[3-(2-Methoxyethoxy)propyl]ureido-6-tridecyl-4[1*H*]pyrimidinone (1d). Activated pyrimidinone **3** (1.55 g, 4.0 mmol) and 3-(2-methoxyethoxy)propyl amine 2d (0.955 g, 7.2 mmol) were added to dry $CHCl_3$ (15 mL) and stirred at 60 °C for 2 days. After cooling to room temperature, 150 mL of $CHCl_3$ was added, and the mixture was extracted 3 times with 60 mL of aqueous 0.1 M HCl (aq), neutralized with 150 mL of saturated $NaHCO_3$ (aq), and washed with 150 mL of brine. After drying with $MgSO_4$ the solvent was removed by evaporation *in vacuo*, resulting in the crude ureido-pyrimidinone (1.53 g, 3.4 mmol). Further purification by recrystallization from 2-propanol, resulted in pure **1d** as a white powder (0.958 g, 2.1 mmol), mp 92.9−93.4 °C Yield: 53%. ^{1}H NMR ($CDCl_3$): δ 13.14 (s, 1H, NH), 11.90 (s, 1H, NH), 10.21 (s, 1H, NH), 5.79 (s, 1H, O=C-CH=C-CH_2), 3.60−3.52 (m, 6H, O-CH_2-), 3.38 (s, 3H, O-CH_3), 3.36 (m, 2H, NH-CH_2-CH_2), 2.46 (t, 2H, CH=C-CH_2-CH_2), 1.91 (m, 2H, NH-CH_2-CH_2-CH_2-O), 1.63 (m, 2H, CH=C-CH_2-CH_2-CH_2), 1.32−1.21 (m, 20H, -CH_2-), 0.88 (t, 3H, -CH_3). ^{13}C NMR ($CDCl_3$): δ 173.0, 156.7, 154.7, 152.4, 105.8, 72.0, 70.1, 68.9, 59.0, 37.1, 32.7, 31.9, 29.6−28.8 (multiple signals), 27.0, 22.7, 14.1. IR (ATR): ν = 2955, 2921, 2852, 1698, 1662, 1585, 1527, 1469, 1446, 1309, 1258, 1200, 1136, 1112, 1047, 947, 882, 849, 815, 792, 771, 742 cm^{-1}. MALDI-TOF-MS (*m*/*z*): 452.33, obsd 453.38 (MH^+), 475.36 (MNa^+). Anal. Calcd for $C_{24}H_{44}N_4O_4$: C 63.68, H 9.80, N 12.38. Found: C 63.83, H 9.94, N 12.46.

Synthesis of 2-{2-[2-(2-Methoxyethoxy)ethoxy]ethyl}ureido-6-tridecyl-4[1*H*] pyrimidinone (1e). Activated pyrimidinone **3** (1.04 g, 2.68 mmol) and 2-(2-[2-methoxyethoxy]ethoxy)ethyl amine **2e** (0.889 g, 5.45 mmol) were added to dry $CHCl_3$ (9 mL) and stirred at 60 °C for 2 days. After cooling to room temperature, 25 mL of $CHCl_3$ was added, and the mixture was extracted 3 times with 10 mL of 0.1 M aqueous HCl, neutralized with 15 mL of saturated $NaHCO_3$ (aq), and washed with 20 mL of brine. After drying with $MgSO_4$ the solvent was removed by evaporation *in vacuo*, resulting in the crude ureidopyrimidinone (1.1 g, 2.3 mmol). Further purification by recrystallization from 2-propanol, resulted in pure **1e** as a white powder (0.89 g, 1.8 mmol), mp 82.6−83.0 °C. Yield: 69%. ^{1}H NMR ($CDCl_3$): δ 13.08 (s, 1H, NH), 11.93 (s, 1H, NH), 10.28 (s, 1H, NH), 5.80 (s, 1H, O=C-CH=C-CH_2), 3.64 (m, 8H, O-CH_2-), 3.52−3.47 (m, 4H, O-CH_2- + NH-CH_2-), 3.35 (s, 3H, O-CH_3), 2.45 (t, 2H, CH=C-CH_2-CH_2), 1.63 (m, 2H, CH=C-CH_2-CH_2-CH_2), 1.28 (m, 20H, -CH_2-), 0.87 (t, 3H, -CH_3). ^{13}C NMR ($CDCl_3$): δ 173.0, 156.8, 154.6, 152.4, 105.8, 72.0, 70.5, 70.3, 69.4, 59.0, 39.5, 32.7, 31.9, 29.6−28.8 (multiple signals), 27.0, 22.7, 14.1. IR (ATR): ν = 3216, 3135, 3030, 2955, 2918, 2873, 2853, 2817, 1702, 1676, 1641, 1620, 1594, 1562, 1470, 1456, 1418, 1400, 1333, 1280, 1262, 1202, 1186, 1122, 1045, 1028, 997, 982, 949, 937, 925, 866, 854, 827, 799, 791, 780, 772, 767, 742, 720, 708, 694 cm^{-1}. MALDI-TOF-MS (*m*/*z*): 482.35, obsd 483.37 (MH^+), 505.34 (MNa^+). Anal. Calcd for $C_{25}H_{46}N_4O_5$: C 62.21, H 9.61, N 11.61. Found: C 62.51, H 9.69, N 11.70.

Synthesis of 2-{3-[2-(2-Methoxyethoxy)ethoxy]propyl}ureido-6-tridecyl-4[1*H*] pyrimidinone (1f). Activated pyrimidinone **3** (1.55 g, 4.00 mmol) and 3-(2-[2-methoxyethoxy]ethoxy)propyl amine **2f** (0.90 g, 5.08 mmol) were added to dry $CHCl_3$ (13 mL) and stirred at 60 °C for 2 days. After cooling to room temperature, 35 mL of $CHCl_3$ was added, and the mixture was extracted 3 times with 15 mL of 0.1 aqueous M HCl, neutralized with 20 mL of saturated $NaHCO_3$ (aq), and washed with 20 mL of brine. After drying with $MgSO_4$ the solvent was removed by evaporation *in vacuo*, resulting in the crude ureidopyrimidinone (1.6 g, 3.2 mmol). Further purification by recrystallization from 2-propanol, resulted in pure **1f** as a white powder (1.3 g, 2.6 mmol), mp 71.1−74.5 °C. Yield: 65%. ^{1}H NMR ($CDCl_3$): δ 13.14 (s, 1H, NH), 11.91 (s, 1H, NH), 10.20 (s, 1H, NH), 5.81 (s, 1H, O=C-CH=C-CH_2), 3.67−3.52 (m, 10H, O-CH_2-), 3.38 (s, 3H, O-CH_3), 3.33 (m, 2H, NH-CH_2-CH2), 2.46 (t, 2H, CH=C-CH_2-CH_2), 1.90 (m, 2H, NH-CH_2-CH_2-CH_2-O), 1.63 (m, 2H, CH=C-CH_2-CH_2-CH_2), 1.31−1.26 (m, 20H, -CH_2-), 0.88 (t, 3H, -CH_3). ^{13}C NMR ($CDCl_3$): δ 173.0, 156.5, 154.5, 152.3, 105.7, 71.8, 70.5, 70.4, 70.1, 68.7, 58.9, 37.0, 32.6, 31.8, 29.5−28.7 (multiple signals), 26.9, 22.5, 14.0. IR (ATR): ν = 2922, 2853, 2817, 1698, 1662, 1585, 1526, 1469, 1445, 1362, 1309, 1259, 1114, 1043, 991, 964, 948, 883, 816, 792, 771, 742 cm^{-1}. Anal. Calcd for $C_{26}H_{48}N_4O_5$: C 62.87, H 9.74, N 11.28. Found: C 62.96, H 9.76, N 11.37. MALDI-TOF-MS (m/z): 496.37, obsd 497.29 (MH^+), 519.26 (MNa^+), 535.24 (MK^+).

Synthesis of 2-{6-[2-(2-Methoxyethoxy)ethoxy]hexyl}ureido-6-tridecyl-4[1*H*]-pyrimidinone (1g). Activated pyrimidinone **3** (0.44 g, 1.13 mmol), 6-[2-(2-methoxyethoxy)ethoxy]hexyl ammonium trifluoroacetate **2g** (0.50 g, 1.58 mmol) and triethylamine (0.18 g, 1.80 mmol) were added to dry $CHCl_3$ (5 mL) and stirred at 55 °C for 2 days. After cooling, 25 mL of $CHCl_3$ was added, and the mixture was extracted 3 times with 10 mL of 0.1 M aqueous HCl, neutralized with 15 mL of saturated $NaHCO_3$ (aq), and washed with 20 mL of brine. After drying with $MgSO_4$ the solvent was removed by evaporation *in vacuo*, resulting in the crude ureidopyrimidinone (0.53 g, 0.99 mmol). This was purified by recrystallization from 2-propanol, yielding the pure product as a white powder (0.46 g, 0.85 mmol), mp 68.3−68.5 °C. Yield: 75%. ^{1}H NMR ($CDCl_3$): δ 13.17 (s, 1H, NH), 11.88 (s, 1H, NH), 10.18 (s, 1H, NH), 5.81 (s, 1H, O=C-CH=C-CH_2), 3.66−3.63 (m, 4H, O-CH_2-), 3.59−3.54 (m, 4H, O-CH_2-), 3.44 (t, 2H, O-CH_2-CH_2-CH_2), 3.38 (s, 3H, O-CH_3), 3.24 (m, 2H, NH-CH_2-CH_2), 2.46 (t, 2H, CH=C-CH_2-CH_2), 1.66−1.54 (m, 6H, NH-CH_2-CH_2-CH_2, O-CH_2-CH_2-CH_2 and CH=C-CH_2-CH_2-CH_2), 1.38−1.26 (m, 24H, -CH_2-), 0.88 (t, 3H, -CH_3). ^{13}C NMR ($CDCl_3$): δ 173.2, 156.6, 154.7, 152.4, 105.8, 72.0, 71.4, 70.7, 70.5, 70.1, 59.0, 40.0, 32.7, 31.9, 29.6−28.9 (multiple signals), 27.0, 26.8, 25.8, 22.7, 14.1. IR (ATR): ν = 2922, 2850, 1698, 1662, 1579, 1526, 1466, 1438, 1307, 1259, 1203, 1124, 1005, 948, 885, 813, 771, 744 cm^{-1}. MALDI-TOF-MS (m/z): 538.42, obsd 539.50 (MH^+), 561.48 (MNa^+), 577.45 (MK^+). Anal. Calcd for $C_{29}H_{54}N_4O_5$: C 64.65, H 10.10, N 10.40. Found: C 64.44, H 10.30, N 10.63.

^{1}H NMR Dilution Experiments and Calculation of K_{dim}. Typical procedure. Weighed amounts of 2-ureido-pyrimidinones **1a**−**g** were dissolved in 2.0 mL of dry $CDCl_3$ (distilled over P_2O_5) resulting in a 10 mM solution, of which 0.6 mL was injected into the NMR tube. The sample was then diluted to 5, 1, 0.5, 0.1, and 0.05 mM (in the case of **1a**−**g**), respectively. The peaks in the alkylidene region were deconvoluted using an algorithm present in the Varian VNMR software. Since the UPy dimer and UPy monomer are in slow exchange on the ^{1}H NMR time scale, it is possible to calculate the molar concentration of dimer and monomer based on the integrals of the NMR signals, the ratio of which is defined as $y = (I_{dimer}/I_{mono})$. From this ratio and the overall UPy concentration U_0, the dimerization constant (K_{dim}) can be calculated using the following equation:

$$K_{dim} = \frac{y(y+1)}{2U_0} \quad (1)$$

The reported errors on the dimerization constant (K_{dim}) have been calculated by averaging of the calculated dimerization constants at the lowest three concentrations. Extreme care was taken to keep water levels in the samples as low as possible, since traces of water could lead to the formation of acid in the solution, which interferes with the hydrogen bonding and can lead to degradation of the model compounds. Therefore, all compounds and glassware were dried over P_2O_5, and $CDCl_3$ was distilled over P_2O_5 and stored over molecular sieves. With this procedure, water levels in the samples were below the detection limit of standard Karl Fischer titrations.

Fourier Transform Infrared Experiments (FT-IR). Infrared (IR) spectra were recorded using a FT-IR spectrometer. Solutions of UPy **1g** and **8** in dry $CDCl_3$ (free of TMS) were loaded between a pair of KBr windows using a 1 mm (for 10^{-3} M solution) or 5 mm (for 10^{-5}−10^{-4} M solutions) Teflon spacer contained in a demountable liquid cell. The absorbance due only to **1g** or **8** was obtained by subtracting the spectra measured for pure $CDCl_3$ under otherwise identical conditions. The resulting corrected spectra were flat in the region between 1800 and 1550 cm^{-1}. For each spectrum, a 128-scan interferogram was collected with 4 cm^{-1} resolution. Measurements were performed without active temperature control.

UV−vis Titrations and Calculation of K_a. UV−vis spectra were recorded using 1 cm path length cells of which the temperature was controlled via a Peltier temperature control system. A series of spectra were obtained by the addition of microliter amounts of a stock solution containing 25.7 μM NaPy **10** and 300 μM UPy (**1e**, **1f**, and **1g**) in dry $CHCl_3$ to a cell containing 2.0 mL of a 25.7 μM solution of 2,7-diamido-1,8-naphthyridine **10** in dry $CHCl_3$ at 25 °C. All obtained traces were baseline-corrected. The association constant of the UPy·NaPy heterocomplex was obtained by nonlinear least-squares analysis of the absorbance at 355 nm as a function of added UPy using a 1:1 binding model accompanied by dimerization of one of the components.[38]

Computational Procedure for DFT and TDDFT Calculations. Geometry optimizations of the 2-ureido-pyrimidinone tautomers **9a**−**c** in the ground state were performed at the B3LYP/6-311+G(d,p) level as implemented in the Gaussian03 package.[32] Previous computational studies have shown that the B3LYP functional gives geometric parameters that are in close agreement with reported crystal structures of UPy dimers.[45] The optimized geometries were confirmed as true minima by vibrational analysis at the same level of theory, as in all cases only real frequencies were found. Geometry optimization was performed using the Berny algorithm, and normal convergence criteria were used (rms force criterion $3*10^{-4}$). All geometries were optimized without symmetry constraints. Given the size of the basis set no BSSE correction was applied for UPy dimers **9a·9a** and **9c·9c**, as this would only produce minor changes, the quality of which would be hard to ascertain. Time-dependent DFT on the optimized geometries of **9a**−**c** was performed using the PBE0 functional in combination with the 6-311++G(2d,p) basis set. The solvent ($CHCl_3$) is taken into account approximately, by employing the polarized continuum model (PCM) based on the integral equation formalism model.[46] Using the PCM approach the solute molecule is placed into a cavity

(45) (a) Guo, D.; Sijbesma, R. P.; Zuilhof, H. P. *Org. Lett.* **2004**, *6*, 3667. (b) Dong, H.; Hua, W.; Li, S. *J. Phys. Chem. A* **2007**, *111*, 2941.

(46) Tomasi, J.; Mennucci, B.; Cancès, E. *J. Mol. Struct.* (*Theochem*) **1999**, *464*, 211.

surrounded by the solvent considered as a continuum medium with certain dielectric constant. The charge distribution of the solute polarizes the dielectric medium, which generates surface charges around the cavity and hence in turn polarizes the solute. In these calculations the so-called nonequilibrium procedure for TDDFT calculations was used, as it has been specifically designed for the study of absorption processes.[33] The oscillator strength of each transition in **9a**−**c** was calculated by the dipole approximation, while visualization of the electronic spectra was achieved using GaussSum.[47]

Geometry optimization of **1c** and **1d** (in their 6[1*H*] tautomeric forms) was started by Monte Carlo conformational searching (using the OPLS 2005 forcefield[48]) of **1c** and **1d** (in which the $C_{13}H_{27}$ chain was replaced with a CH_3 group) with the GB/SA solvation model ($CHCl_3$) as implemented in Macromodel 9.5. In this way 900 structures were generated by varying dihedral angles around all C−C and C−O bonds of the oligoEO chain. In both cases the coordinates of the lowest energy conformer were exported and further optimized at the B3LYP/6-311+G(d,p)//PCM($CHCl_3$) level of theory using the Gaussian03 package.[32] Geometry optimization was performed using direct inversion in the iterative subspace method (GDIIS).[49] The optimized geometries were confirmed as true minima by vibrational analysis at the same level of theory as in all cases only real frequencies were found. In all calculations in which the PCM approach was used to model the effect of solvent, the cavity used for the PCM approach was constructed using the simple united atom topological model (UA0), in which the van der Waals surface was built by placing a sphere around each solute heavy atom while hydrogen atoms were enclosed in the sphere of the atom to which they are bonded.

Acknowledgment. The authors wish to acknowledge Mr. J. van Dongen, Dr. X. Lou, Mr. Ralf Bovee, and Mr. H. Eding for technical assistance. Dr. G. Tew (University of Massachusetts Amherst) and Dr. M. van Genderen are acknowledged for helpful discussions. Dr. E. Pidko is acknowledged for help with the DFT calculations. This work is supported by the Council for Chemical Sciences of The Netherlands Organization for Scientific Research (CW-NWO).

Supporting Information Available: Synthesis of amines **2c**−**2g**; ^{1}H NMR dilution studies in anhydrous $CDCl_3$ on a 1:1 mixture of diethylene glycol dimethyl ether and an UPy compound bearing only aliphatic side chains; NMR spectra; Cartesian coordinates, SCF energies and frequencies for optimized structures at the B3LYP level of theory. This material is available free of charge via the Internet at http://pubs.acs.org.

(47) O'Boyle, N. M.; Tenderholt, A. L; Langner, K. M. *J. Comput. Chem.* **2008**, *29*, 839.
(48) Jorgensen, W. L.; Tirado-Rives, J. *Proc. Natl. Acad. Sci. U.S.A.* **2005**, *102*, 6665.
(49) Csaszar, P.; Pulay, P. *J. Mol. Struct.* **1984**, *114*, 31.